

Numerical investigation of hydrogen consumption in Proton Exchange Membrane Fuel Cell by using computational fluid dynamics (CFD) simulation

Yassine Amadane ^{1,*}, Hamid Mounir ¹, Abdellatif El Marjani ¹, Ettouhami Mohamed Karim ² and Asifa Awan ³

¹ Research Team EMISys, Research Center Engineering 3S, School Mohammadia of Engineers, Mohamed V University of Rabat, Morocco

² Centre de Recherche en Sciences et Technologies de l'Ingénieur et la Santé, ENSET, Mohamed V University of Rabat, Morocco

³ Institute of Chemical Engineering, University of the Punjab, Lahore, Pakistan

Abstract: Proton exchange membrane fuel cell (PEMFC) is the most important system that converts chemical energy into electricity by using hydrogen oxidation and oxygen reduction reactions. With this approach, a 3-D (CFD) thermo-fluid model was studied using a commercial code ANSYS fluent for investigating the performance of the PEMFC system. The developed model can evaluate the distribution of gas species like the mass fraction of hydrogen, as well as the distribution of water in PEMFC. The results are used to investigate the influence of temperature and cell voltage on the consumption of hydrogen from inlet $z=0$ mm to outlet $z=50$ mm. The obtained polarization curve I-V is compared with the literature findings. The analysis shows a good agreement between our findings and the experimental results. The CFD simulation shows that the cell voltage affects considerably the hydrogen consumption; at 333 K, it can be seen that the hydrogen mass fraction decreases from 80% to 67% at 0.7 V and 80% to 73% at 0.9 V. By comparing the hydrogen mass fractions; at a low cell voltage the hydrogen mass fraction dropped by only 7%, while at a high cell voltage the hydrogen mass fraction dropped by about 13% from the inlet to outlet. Consequently; our analyses show high consumption of hydrogen at low cell voltages.

Keywords: PEMFC; consumption; hydrogen; CFD; ANSYS.

Introduction

Proton exchange membrane fuel cells or (PEMFCs) have had a major revolution regarding research aimed at their theoretical understanding and modelling ¹. Proton exchange membrane (PEM) fuel cells are the current focus of research for fuel cell vehicle applications. PEM fuel cells are thus likely to play a key part in green energy economies based essentially on energy efficiency and renewable energy ². Elseways, the architecture of PEM fuel cells is a quite complex (due to lots of input parameters need to be considered when developing PEM fuel cell designs) multi-physics task that is greatly facilitated by a computer simulation modelling incorporating all the necessary theoretical equations. The main advantages of PEMFC when compared to a solid oxide fuel cell (SOFC) and Direct methanol fuel cell (DMFC) is that they have high efficiency and they are also able to operate in low temperatures around 80 °C ³. The use of fuel

cells for automotive applications needs hydrogen technologies⁴. Hydrogen produced from renewable energy sources such as solar and wind energy, stored as a compressed gas, liquid or in the solid state, and then used in fuel cells to produce electricity, offers an attractive, sustainable energy option for transport and stationary applications ⁵. Recently, many researchers have been investigated and developed a thermo-fluid model of a proton exchange membrane fuel cell with a straight flow channel. Many papers have been studied the single-channel design of PEMFC to analyze the distribution of gas species (H₂ and O₂) and especially the hydrogen consumption along the anode channel. A three-dimensional model to study the influence of different parameters on (PEM) fuel cell performance (geometry, materials) is simulated and presented by Sadiq Al-Baghdadi and Shahad Al-Janabi ⁶. Lin et al ⁷. showed the dependence between the mass fraction of oxygen and the overpotential.

*Corresponding author : Yassine Amadane

Email address : yassineamadane@research.emi.ac.ma

DOI: <http://dx.doi.org/10.13171/mjc7618121415ya>

Received September 25, 2018

Accepted November 3, 2018

Published December 14, 2018

Tolj et al.⁸ studied the PEMFC performance for non-uniform temperature, the single cell was divided into five equal parts, and the experimental results have shown significant improvement when compared to the isothermal case. Hinatsu et al.⁹ have proposed a model for membrane water by changing the temperature from 25° to 130°. Ozden et al.¹⁰ proposed a three-dimensional computational fluid dynamics model from Tolj et al.⁸. In the study of Hashemi et al.¹¹ a comprehensive non-isothermal model has been established to investigate the performance of PEMFC with straight and serpentine flow fields. The model considers the major electrochemical phenomena, oxygen and hydrogen mass fractions distribution. In Mahayri's paper¹² a transient multiphase in a dead end anode model is investigated for modelling and simulation. In H. Kazemi Esfeh et al.'s paper¹³ a CFD model of a serpentine PEMFC was carried out.

The use of the ANSYS module to simulate our PEMFC with a single flow channel is presented. The main objective of this study is to understand the consumption of hydrogen of a PEMFC with a single flow channel. The ANSYS model has been created to analyze the mass fraction of hydrogen and water. The consumption of hydrogen along the anode channel was discussed. Our model is also used to investigate the impact of changing the voltage on the hydrogen consumption and water dynamics.

A fuel cell is a system that uses hydrogen and oxygen to produce electricity by an electrochemical reaction, as shown in (Fig.1). There are different types of fuel cells, such as Alkaline Fuel Cell (AFC), Solid Oxide Fuel Cell(SOFC), Proton Exchange Membrane Fuel Cell (PEMFC), Molten Carbonate Fuel Cell (MCFC) etc. The classification these types based on the type of electrolyte¹. In this paper, we will focus our study on the proton exchange membrane fuel cell.

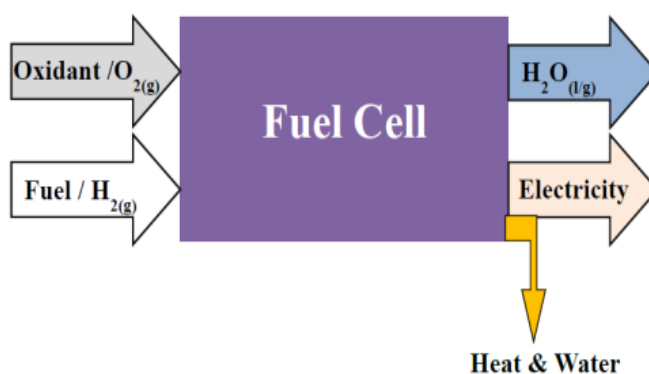


Figure 1. Schematic of the fuel cell system.

Mathematical model

A 3-D finite element model was created using ANSYS code and taking into account phenomena

involving transport in the membrane, GDL, catalyst layer. The description of PEMFC is presented in (Fig. 2)¹⁴.

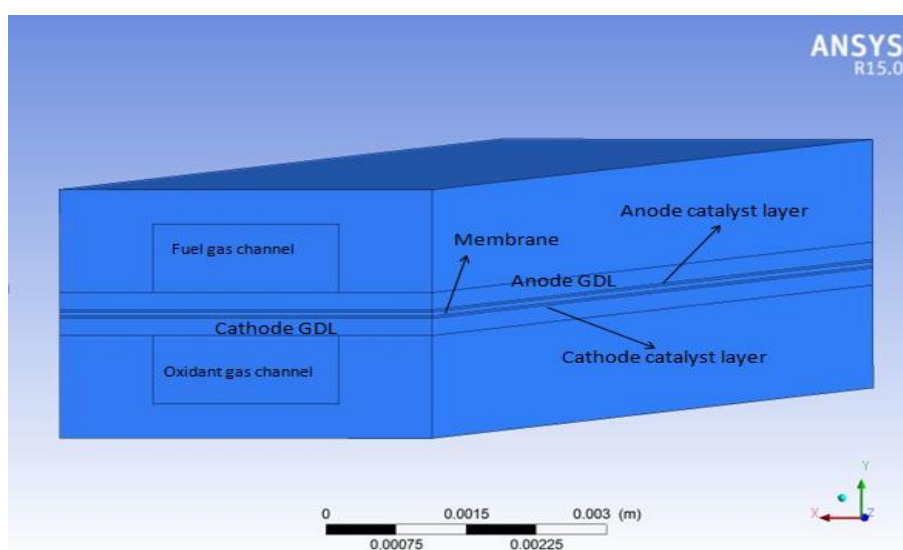


Figure 2. Description of PEM fuel cell

Hydrogen gas passes into the anode side. It diffuses through the (GDL) and reaches the catalyst layer (CL), where it forms ions and electrons. The hydrogen ions diffuse through the membrane, and electrons flow through the anode (GDL) to the current collectors (CC). The electrons enter the cathode side through the current collectors and the gas diffusion layer. Upon reaching the cathode

catalyst layer, the electrons, hydrogen ions and oxygen combine to form water and release heat ¹⁵.

The elementary PEM fuel cell consists of two catalyst layers, two gas diffusion layers, current collectors and membrane ¹⁶. The PEM fuel cell components are summarized in (Table. 1).

Table 1. (PEMFC) components and materials.

PEMFC parts	Materials	Properties
Current collectors	Gold plating	High electrical and thermal conductivities.
Catalyst Layers	Platinum	Performs electrochemical reaction
Gas diffusion layers	Carbon fiber	Conduct electrons between the bipolar plate and electrode
Membrane	Nafion	Transfer protons

The governing equations are formulated under the following assumptions ¹¹:

Assumptions:
Steady-state system
Isothermal condition (temperature constant)
The flow is laminar
GDL: Isotropic and homogeneous
Activation over potentials: Constant within anode and cathode
Incompressible fluids
Bulter-Volmer equations for electrochemical reaction

All simulations presented in this work are performed by using ANSYS-Fluent software 15.0.

The four basic steps of our simulation study are presented in Fig.3:

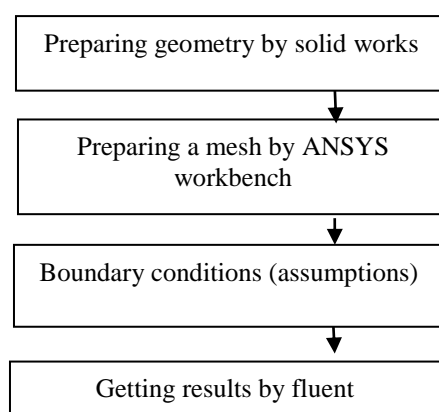


Figure 3. Steps of modelling

Thermo fluid model

Thermo-fluid model – Governing equations

This section described the governing transport equations used for this research work. These governing equations were selected by the literature review of the work done by a different researcher. The fluid and temperature fields in the whole domain are obtained by solving the steady-state Navier-Stokes equations, consisting of the continuity equation, the momentum equations and the mass conservation equation for each species, and the energy conservation equation:

- Continuity equation:

This equation represents the mass conservation for all transport phenomena that take place in the fuel cell, and it is described as:

$$\nabla(\rho\vec{u})=S_m \quad (1)$$

Where ρ is the density.

- Momentum conservation:

The momentum transport equation in a steady-state is written as:

$$\nabla(\rho\vec{u}\vec{u}) = -\nabla p + \nabla(\mu\nabla\vec{u}) + S_u \quad (2)$$

Where p is the pressure

- Species conservation:

The species transport equation represents the mass conservation for all gas species, and it is defined as:

$$\nabla(\vec{u}C_i) = \nabla(D_i^{eff} \nabla C_i) + S_i \quad (3)$$

Where D_i^{eff} is the effective diffusivity

- Energy conservation:

The energy equation is written as:

$$\nabla(\rho C_p \vec{u}T) = \nabla(k^{eff} \nabla T) + S_T \quad (4)$$

Where k^{eff} is the effective thermal conductivity

All the source terms appearing in the governing equations are:

S_m : Source term for continuity equation.

S_u : Source term for momentum equation.

S_i : Source term for the species inside catalyst layers.

S_T : Source term for the energy equation.

Electrochemical model

The fluid dynamics equations are coupled at the electrochemical model implemented in ANSYS-Fluent.

$$\nabla(\sigma_m^{eff} \nabla \Phi_m) + R_m = 0 \quad (5)$$

Equation (5) associated with the protons transport the membrane and catalyst layers

$$\nabla(\sigma_s^{eff} \nabla \Phi_s) + R_s = 0 \quad (6)$$

Equation (6) associated with the electrons transport in catalyst layers and gas diffusion layers. Where σ is the electric or ionic conductivity, Φ is the cell potential and R is the transfer current. The transfer current and source terms are determined from the general Butler-Volmer formulation.

The membrane is simulated as a porous zone, and its properties as ionic conductivity σ_m and the electro-osmotic drag coefficient are expressed as a function of the water content λ ¹⁸.

$$\sigma_m = (0.00514\lambda - 0.00326) \exp(1268(1/300 - 1/T)) \quad (7)$$

$$\lambda = 0.043 + 17.81a - 39.84a^2 + 36a^3 (a < 1) \quad (8)$$

$$\lambda = 14 + 1.4(a-1)(a > 1) \quad (9)$$

Where a is the water activity. This model is used to simulate the formation and transport of water in the fuel cell.

Boundary conditions

In the current study, there are two types of external boundary conditions. We used the following equations to illustrate the boundary conditions as shown in (Table. 2)¹⁷.

Source terms

Table 2. Boundary conditions.

In the region of the anode $\Phi_s = 0$	$\frac{\partial \Phi_M}{\partial y} = 0$
In the region of the cathode	$\Phi_s = V_{Cell}$ $\frac{\partial \Phi_M}{\partial y} = 0$
In the region of exterior boundaries	$\frac{\partial \Phi_M}{\partial x} = 0, \frac{\partial \Phi_M}{\partial z} = 0, \frac{\partial \Phi_s}{\partial x} = 0, \frac{\partial \Phi_s}{\partial z} = 0$

Details of calculations

Geometrical modelling

The design of our system in ANSYS is presented in (Fig.4). The geometry modelled is a 2.9 mm * 4 mm * 50 mm. The anode side is for hydrogen, and the cathode side is for oxygen or

air. The gas channel is 4 mm wide and 2 mm high. The thicknesses of the membrane, gas diffusion layer, catalyst layer are 0.15 mm, 0.3 and 0.02 mm respectively as shown in (Table. 3).

Table 3. (PEM) fuel cell dimensions.

Part	Length	Width	Height	Unit
Gas channels	50	2	1	mm
Gas diffusion layer	50	4	0.3	mm
Catalyst layer	50	4	0.02	mm
Membrane	50	4	0.15	mm
Current collector	50	4	1.5	mm

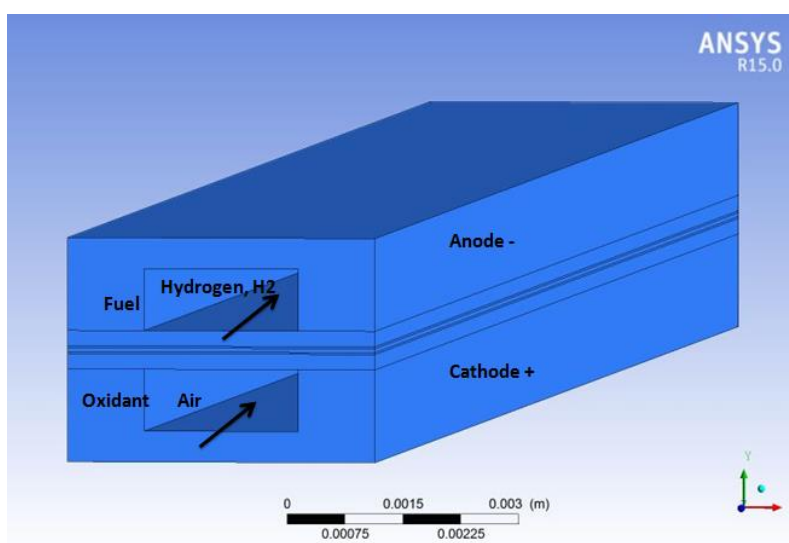


Figure 4. Schematic of PEMFC geometry

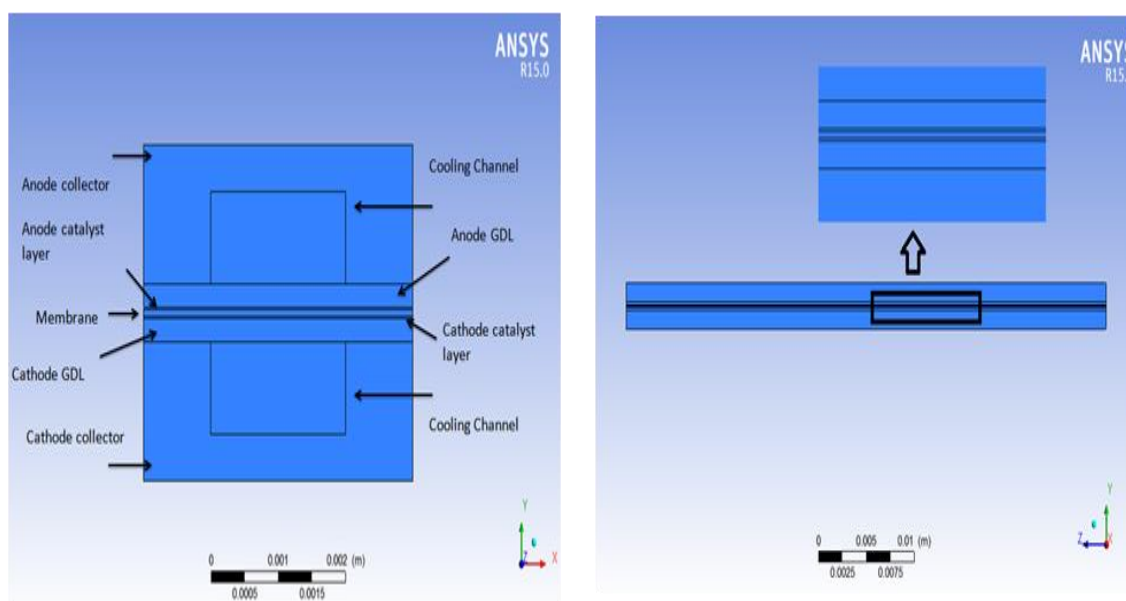


Figure 5. Schematic of a PEMFC: (a) XY plane, (b) YZ plane

The basic case of a PEM fuel cell with a single straight gas flow channel on each side of the (MEA), the upper plate for hydrogen and the lower plate for air or oxygen, is presented in (Fig. 4) and (Fig. 5).

Algorithm resolution

The thermo-fluid model was studied using the ANSYS 15.0 code. This numerical code has an add-

on module for fuel cells. A simple algorithm is used for solving equations (the mass, momentum and energy).

The number of iterations was determined as 1800. TOSHIBA-PC-Intel® Core (TM) i3-310M CPU @2.4 GHz, 2.4 GHz was used to solve the problem.

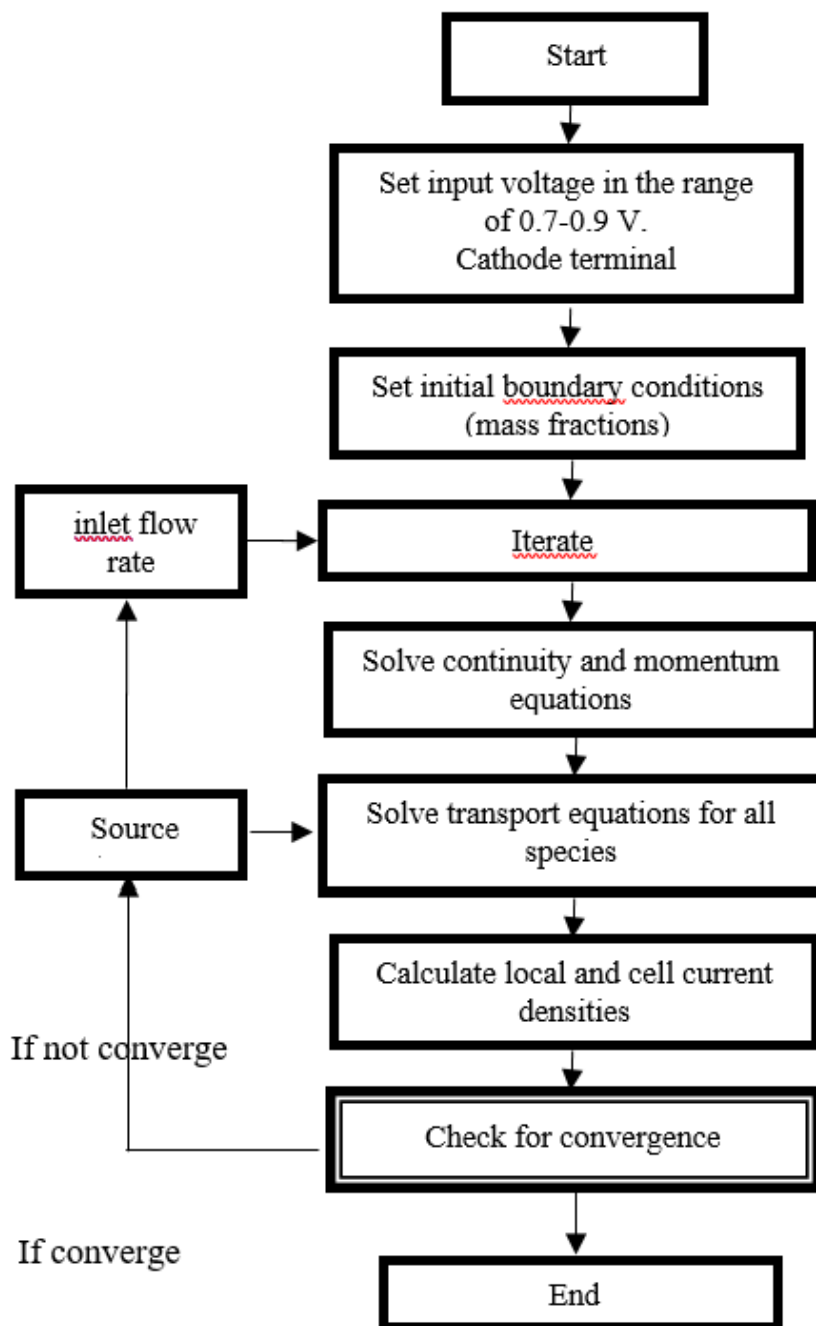


Figure 6. Solution algorithm used in Fluent

Parameters values

The numerical calculations are performed to evaluate the temperature and voltage influences on the hydrogen consumption in (PEMFC). The simulation takes about one hour for completing

1200 iterations. The boundary conditions of our iso-thermal model and the physical parameters are presented in the (Table. 4) and (Table. 5) respectively

Table 4. Boundary conditions of our model.

Boundary Conditions	Location		Values	Units
Velocity inlet	Inlet Anode	Inlet gas velocity	0.3	m/s
		Inlet hydrogen mass fraction	0.8	-
		Inlet water mass fraction	0.2	-
	Inlet Cathode	Inlet gas velocity	0.5	m/s
		Inlet oxygen mass fraction	0.9	-
		Inlet water mass fraction	0.1	-
Pressure Outlet	Outlet Anode	Outlet gas pressure	0	Pa
	Outlet Cathode	Outlet gas pressure	0	Pa
Wall	Terminal Anode	Specified electric potential	0	V
	Terminal Cathode	Specified electric potential	0.7-0.9	V
	All faces	Constant temperature	343	K

Table 5. parameters values.

Description	Value	Dimension
Channel length	50	mm
Cell width	2.9	mm
Cell height	4	mm
Cell temperature	333/343/353	K
Anode pressure	2	Pa
Cathode pressure	2	Pa
Concentration exponent	0.5	-
Open circuit voltage	0.95	volts
Exchange coefficient	2	-
Mass flow rate (Anode)	10^{-6}	kg/s
Mass Flow rate (Cathode)	10^{-5}	kg/s
Equivalent weight (membrane)	1100	kg/kmol
Protonic conduction (coefficient and exponent)	1	-

The operating pressure of the H₂ inlet is 1 bar gauge, with a 0.8 mass fraction for H₂, and 0.2 for water. The operating pressure of the O₂ inlet is 1 bar gauge, with a mass fraction of 0.9 for O₂, and 0.1 for water.

In the next section, we will present a simulation of a single PEMFC by using ANSYS Fuel Cell Module.

Results and Discussion Thermo-fluid model validation

Table 6. Comparison of the current density of experiment and simulation

Our model		Experimental data ¹⁹		Difference of current densities	Percentage
Current density(A/cm ²)	Voltage(V)	Current density(A/cm ²)	Voltage(V)		
0.884657	0.7	0.78	0.7	0.104657	13.41%
0.372922	0.8	0.33	0.8	0.043922	13.30%
0.143458	0.85	0.12	0.85	0.023458	19.54%
0.027492	0.9	0.022	0.9	0.005492	24.96 %

By comparing the difference of current densities as shown in (Table. 6), at 0.9 V the current density of our model was higher than the experiment by 24.96 %.

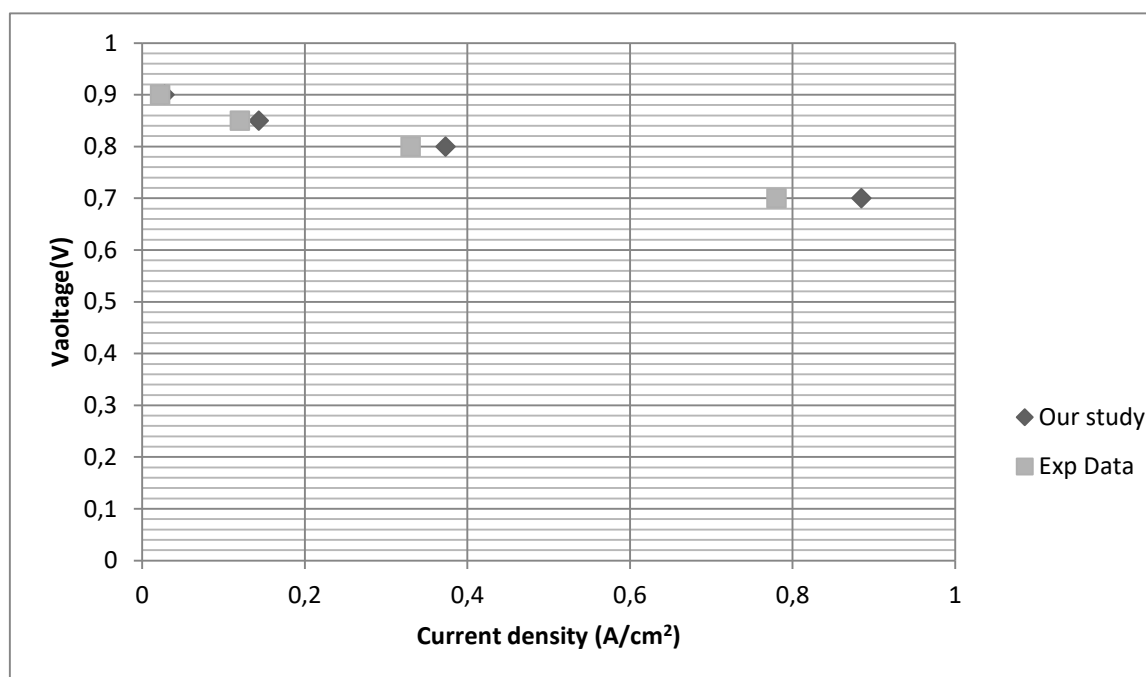


Figure 7. Validation of thermo-fluid model¹⁹

Fig.7 represents the comparison between our numerical findings and experimental results¹⁹. The maximum current densities: 0.884657A/cm² at 0.7 V for the present model, 0.78 A/cm² at 0.7 V for experiment. In the middle range of voltage, the current densities of the present work were similar

than the experiment. Our study presented the result in a reasonable range of the real PEM fuel cell.

In the following subsection, the hydrogen mass fraction distribution will be discussed. The temperature and voltage were varied 333 K, 343 K and 353 K at 0.7 V and 0.9 V respectively.

Distribution of hydrogen's mass fraction in PEMFC

For 333 K

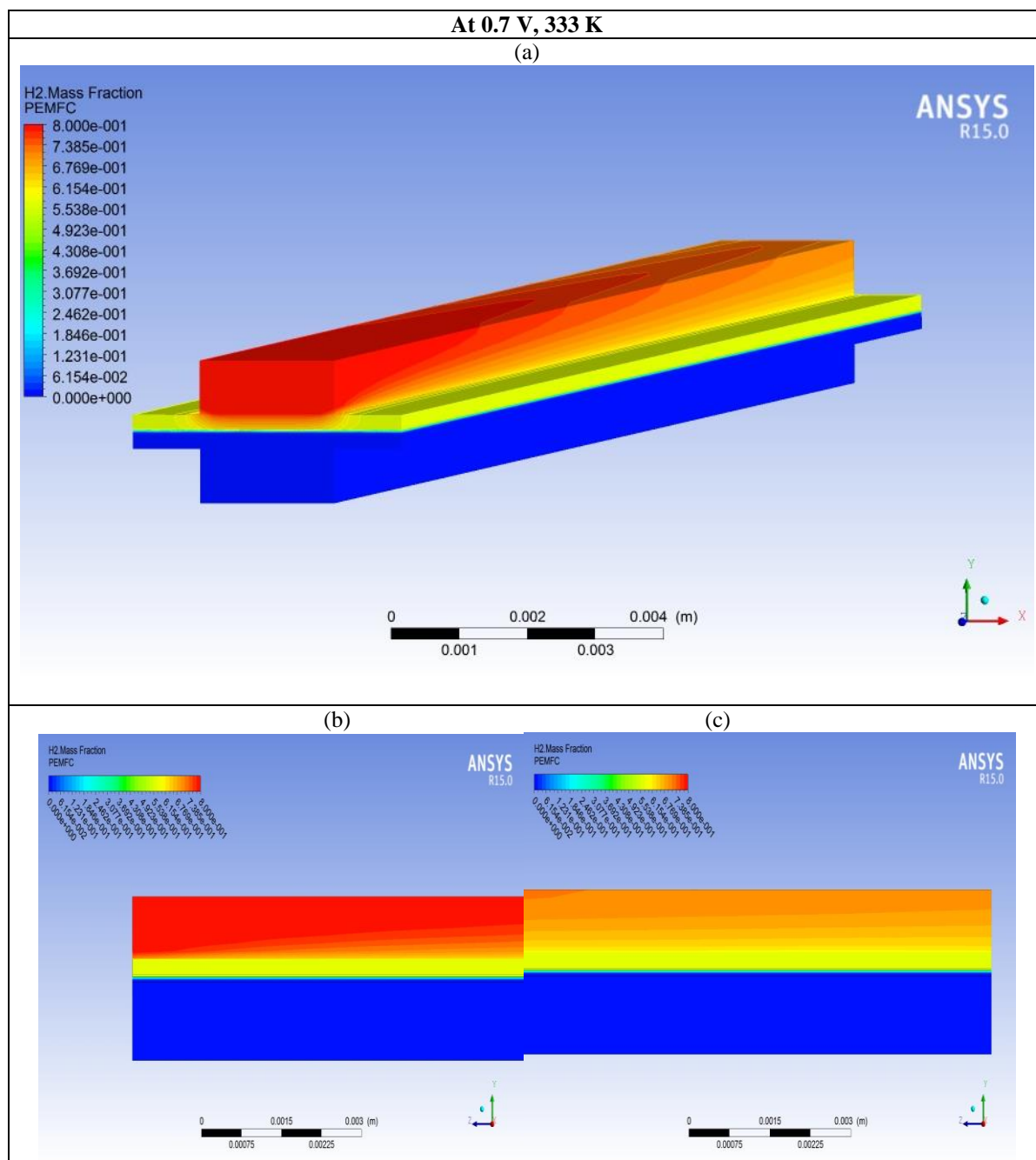


Figure 8. Three-dimensional distribution of hydrogen mass fraction at anode side: (a) Three-dimensional model, (b) The beginning of the anode channel, (c) the end of the anode channel, 333K.

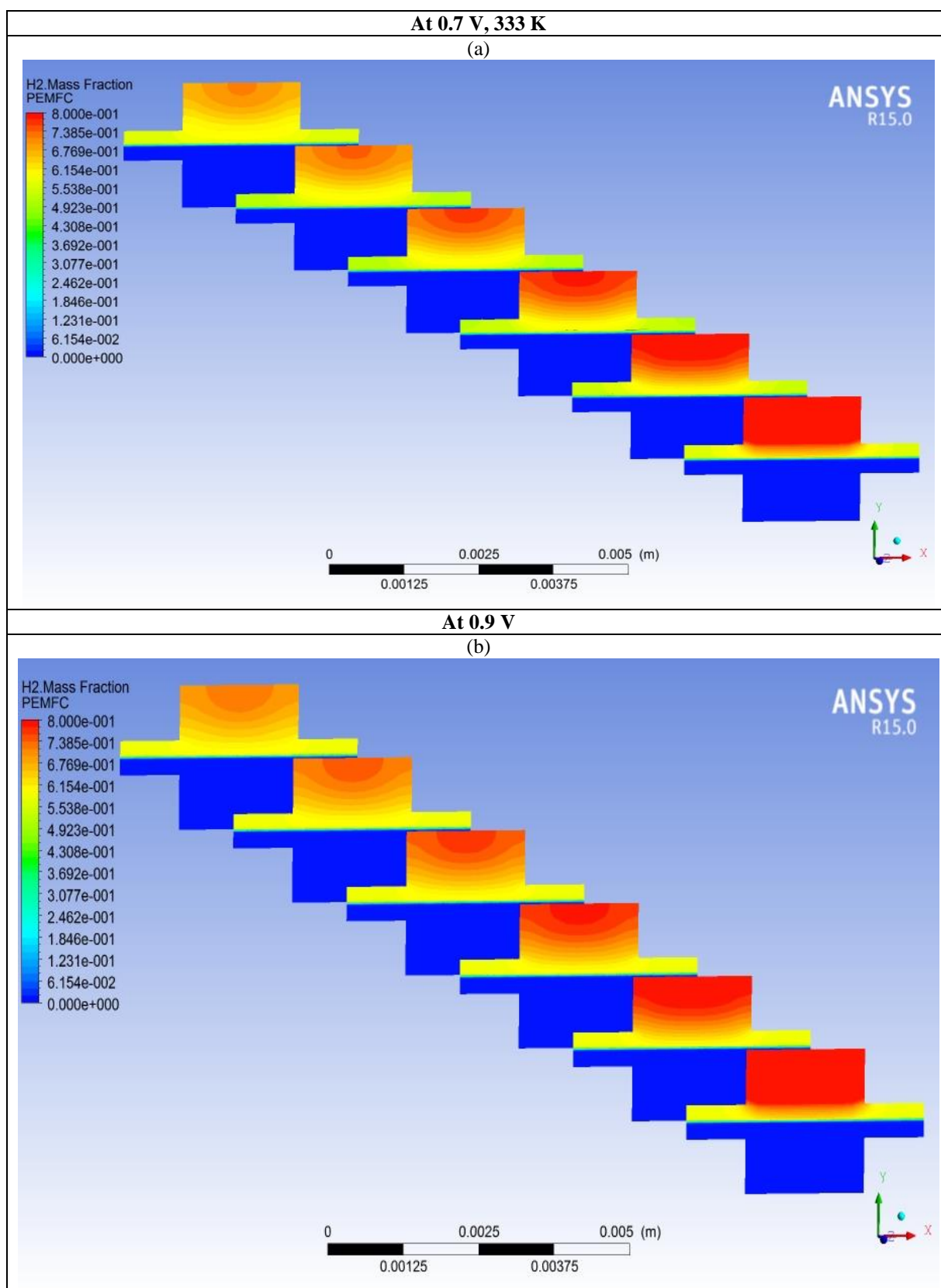


Figure 9. Hydrogen mass fraction distribution in PEMFC, (a) 0.7 V and (b) 0.9 V at $T=333$ K. For six planes $z = 0.0$ mm, $z = 10$ mm, $z = 20$ mm, $z = 30$ mm, $z = 40$ mm and $z = 50$ mm.

It is very important to know the hydrogen transport along the anode side in order to improve the performance of (PEM) fuel cell. Fig. 8 shows the

three-dimensional contour of the mass fraction of hydrogen at the anode channel.

In (Fig. 9(b)) showing the hydrogen distribution in the y-z plane at 333 K, the hydrogen mass fraction decreased along the flow channel. This decrease of hydrogen mass fraction along the anode channel was caused by the hydrogen consumption at $V=0.7$ V ^{20, 21, 22}.

Our simulation results are generated with two cell voltages of 0.7 V and 0.9 V. At 333 K, it can be seen in (Fig. 9(a) and (b)) that the hydrogen mass fraction decreases from 80% to 67% at 0.7 V and from 80% to 73 % at 0.9V.

The mass fraction of hydrogen decreases along z-direction because hydrogen is consumed from $z=0$ mm to $z=50$ mm. The hydrogen is oxidized to give two hydrogen ions ($2H^+$) and two electrons ($2e^-$) (oxidation reaction) at the anode catalyst layer and the membrane. On the other hand, the oxygen recombines with hydrogen ions to form water and heat at the cathode catalyst layer and membrane ^{23, 24, 30}.

For 343 K

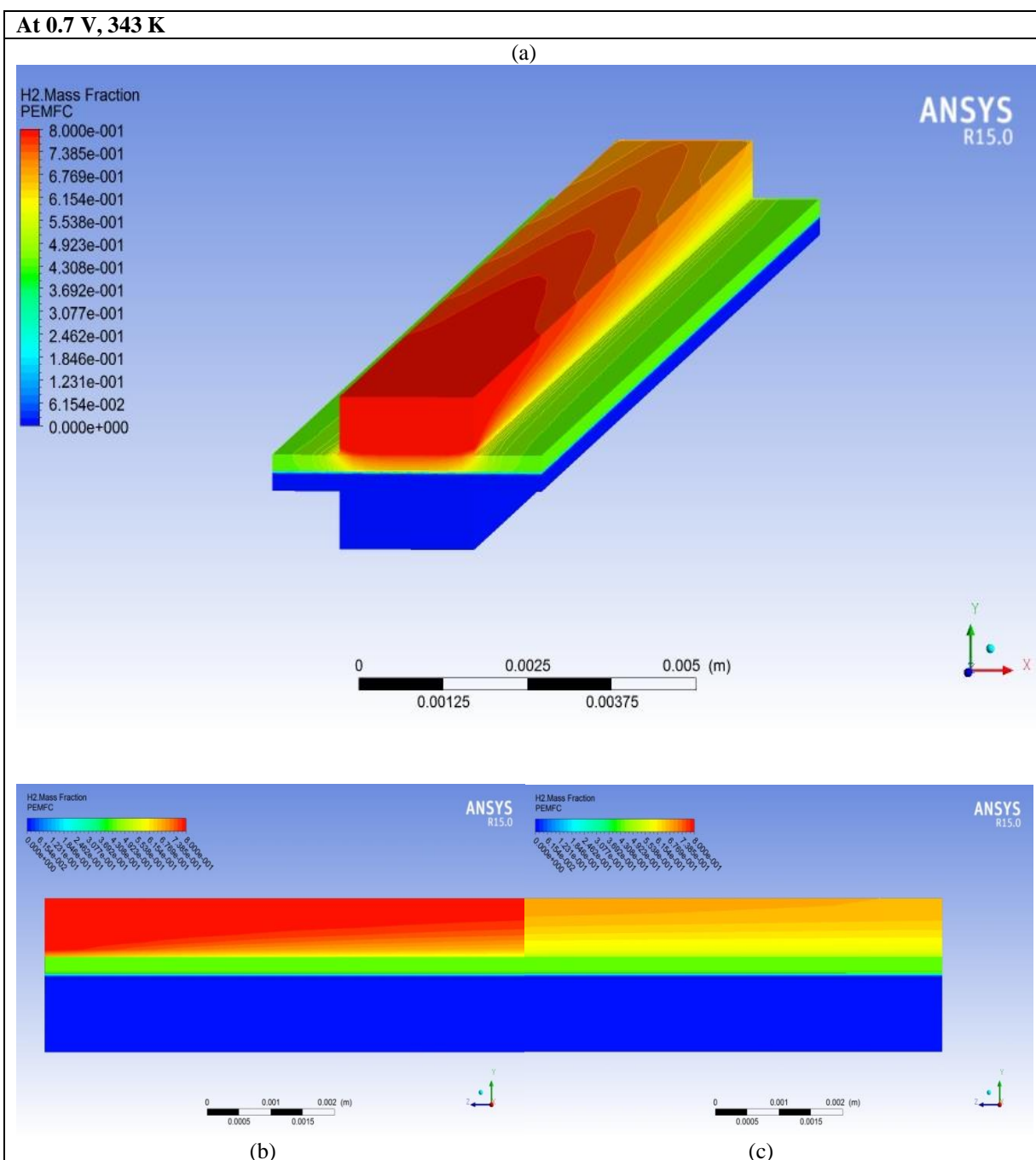


Figure 10. H₂ mass fraction distribution in the anode channel: (a) Three-dimensional model, (b) The

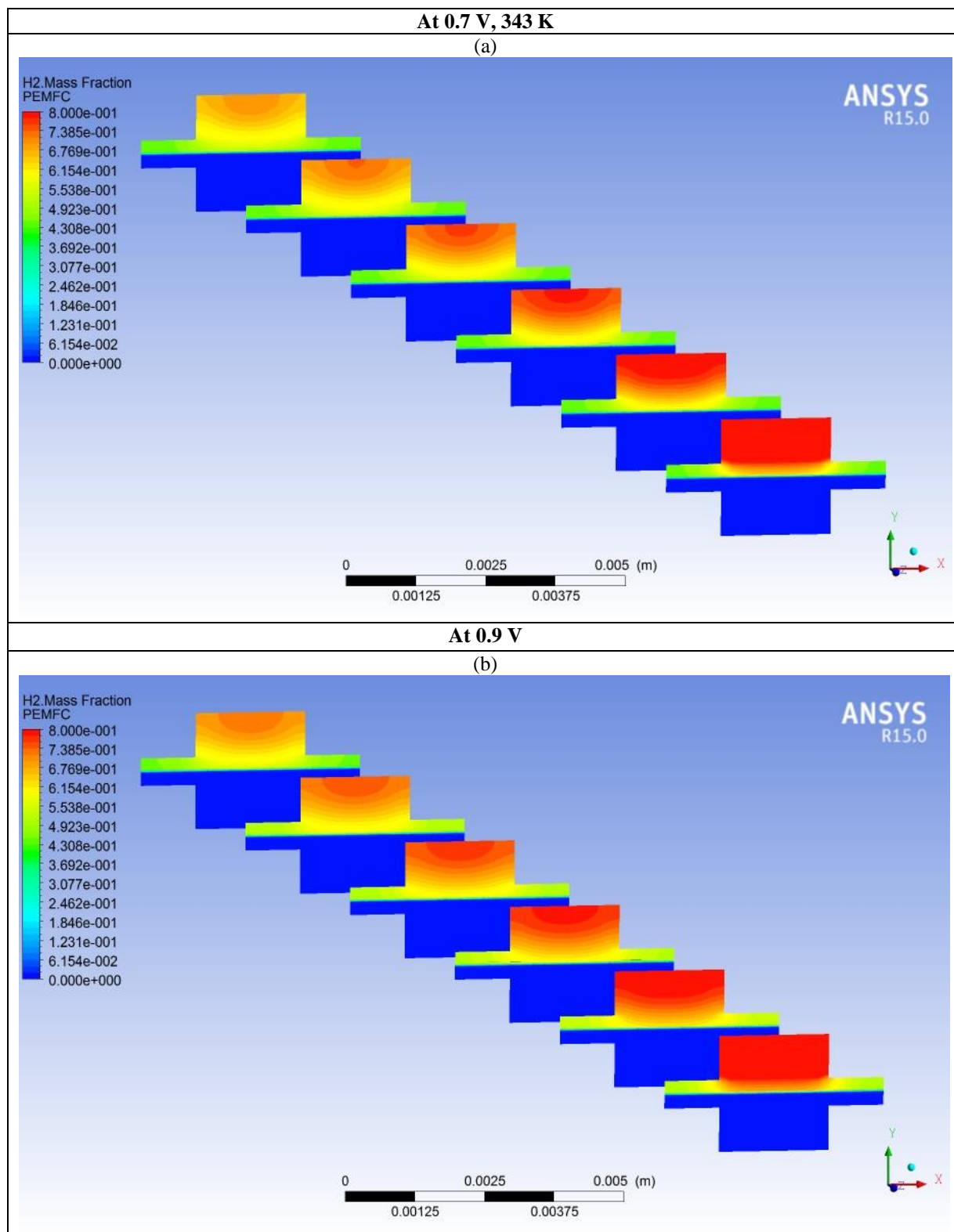


Figure 11. H₂ mass fraction distribution in PEMFC, (a) 0.7 V and (b) 0.9 V at T=343 K. For six planes from z= 0 mm to z=50 mm.

For 353 K

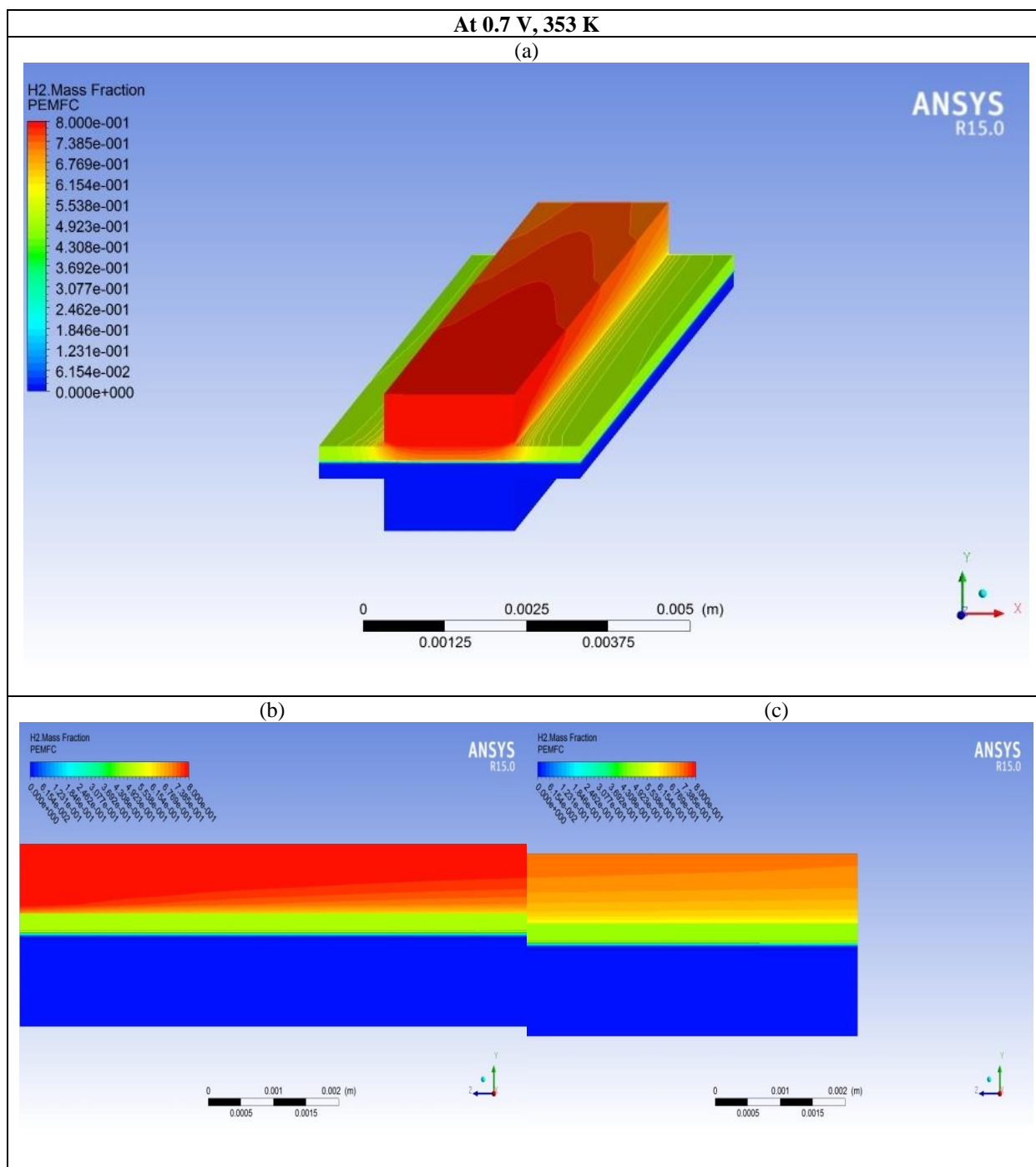


Figure 12. H₂ mass fraction distribution in the anode channel: (a) Three-dimensional model, (b) The beginning of the anode channel, (c) The end of the anode channel, 353 K.

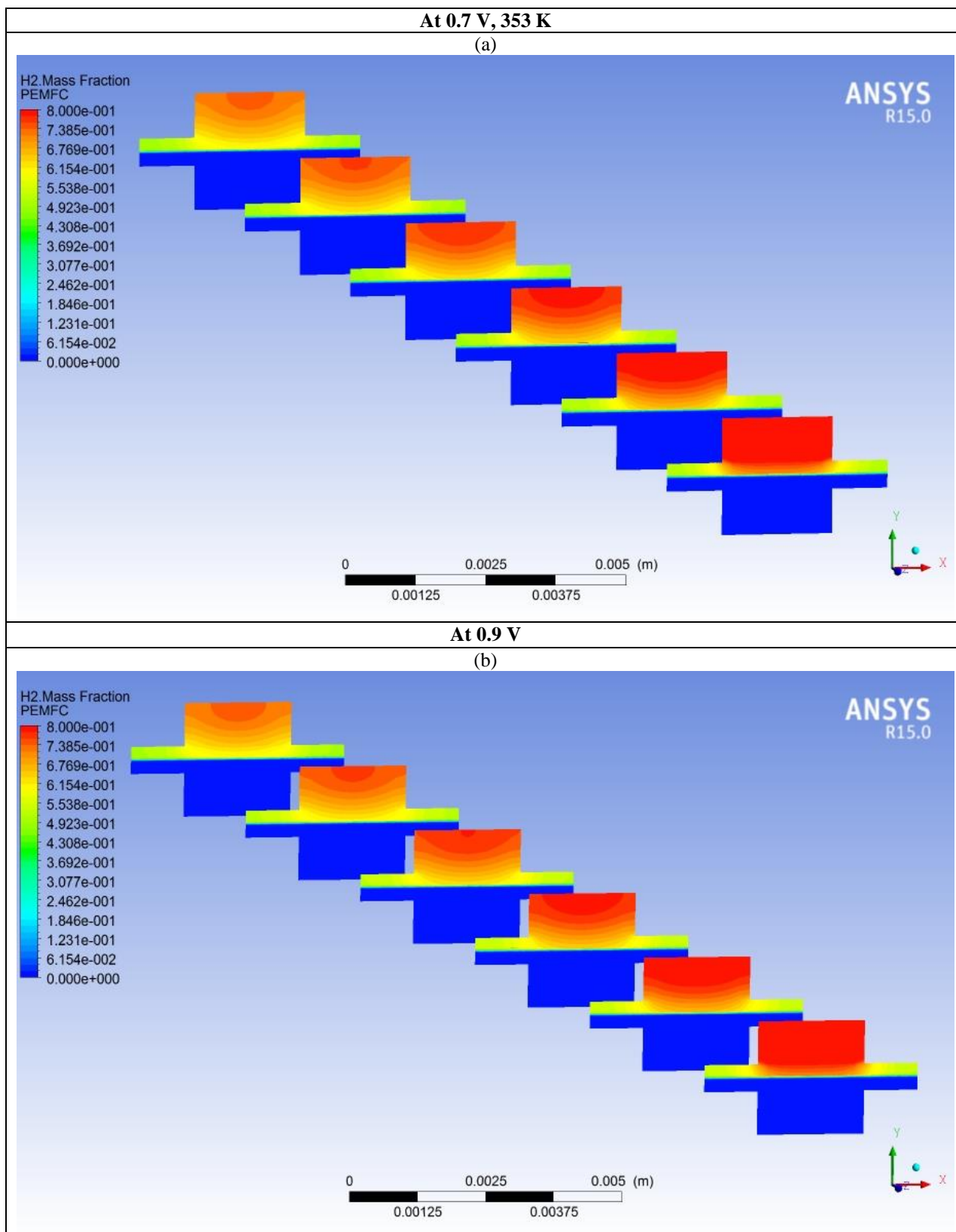


Figure 13: H₂ mass fraction distribution in PEMFC, (a) 0.7 V and (b) 0.9 V at T=353 K. For six planes from z= 0 mm to z=50 mm.

(Fig.10) shows the evolution of hydrogen mass fraction along the anode side of the single PEM fuel cell at V = 0.7 V. 3D numerical analysis investigating the distribution of hydrogen along the

anode channel show a decrease in hydrogen mass fraction (in the flow direction).

(Fig. 11) represents the hydrogen mass fraction evolution along the anode channel for six planes

($z=0.0$ mm, $z=10$ mm, $z=20$, $z=30$ mm, $z=40$ mm, and $z=50$ mm) of the single PEM fuel cell at 0.7 V and 0.9 V.

At 343 K, as observed in (Fig. 11 (a) and (b)), the hydrogen mass fraction is at a maximum of 80% at the inlet and decreases gradually to 61% for 0.7 V and from 80% to 67 % for 0.9 V.

At 353 K, the hydrogen mass fraction shows no significant change from $z = 0$ mm to $z = 50$ mm for 0.7V and 0.9 V. The hydrogen enters the anode side at a maximum mass fraction of 80 % and exits at a mass fraction of 72 %. There is a gradient of 8% in hydrogen mass fraction across this flow channel.

Our study shows a high consumption of hydrogen at low voltages; consequently, the higher amounts of water are consumed at low cell voltages to keep the membrane wet^{25,26}. Depending on the hydration state of the membrane, proton migration is associated with a drag of water molecules from the anode to the cathode side. The electro-osmotic drag transport, together with electrochemical water production, results in an accumulation of water at the cathode side. In turn, the water concentration gradient between the anode and cathode causes back diffusion, which works against drying of the membrane from the anode side¹⁸.

Distribution of water mass fraction and relative humidity in PEMFC

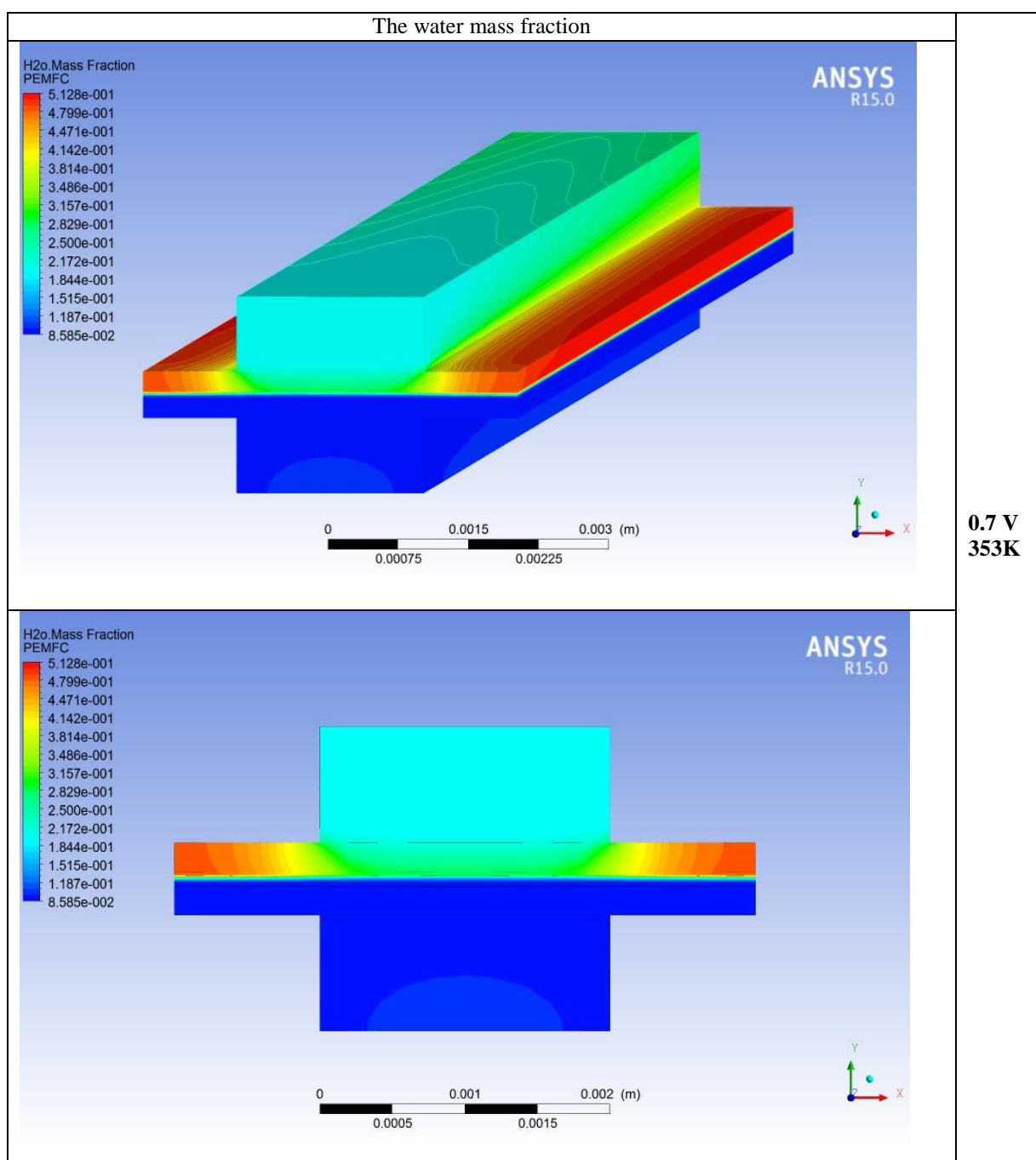


Figure 14. Water mass fraction distribution at 353 K, 0.7 V .

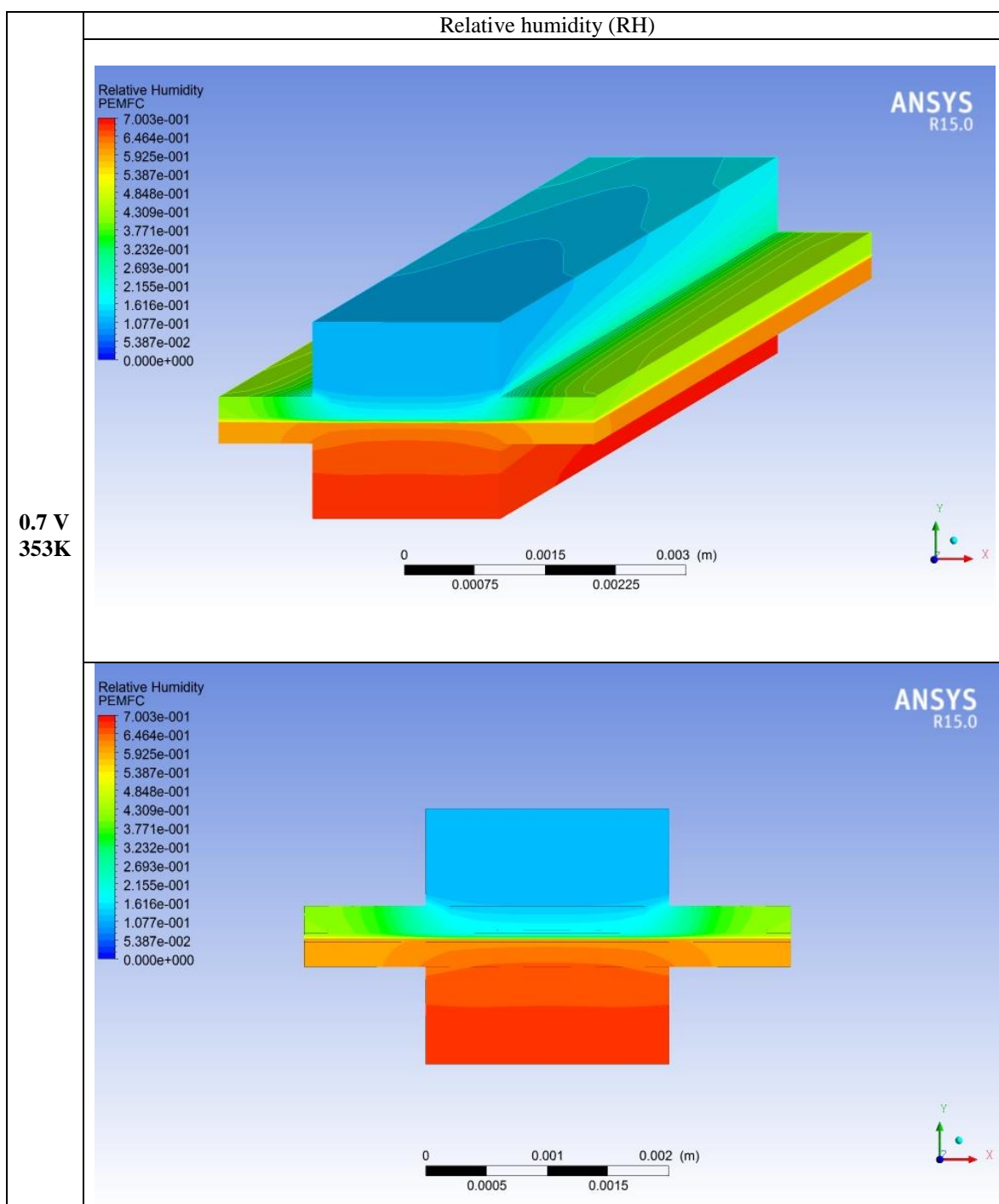


Figure 15. Relative humidity at 353 K, 0.7 V.

A comparison of the water mass fraction distribution and relative humidity at low voltage is presented in (Fig. 14) and (Fig. 15).

It can be seen in Fig. 14 that the water mass fraction at the inlet of the channel is 0.18 and increases to 0.28 as flows reach the outlet. The highest values of water mass fraction, 0.51, are

found in the gas diffusion layer (GDL) where the reaction takes place.

Fig. 15 shows that the relative humidity is very higher in the cathode channel, cathode gas diffusion layer, membrane than in the anode regions^{27,28,30}.

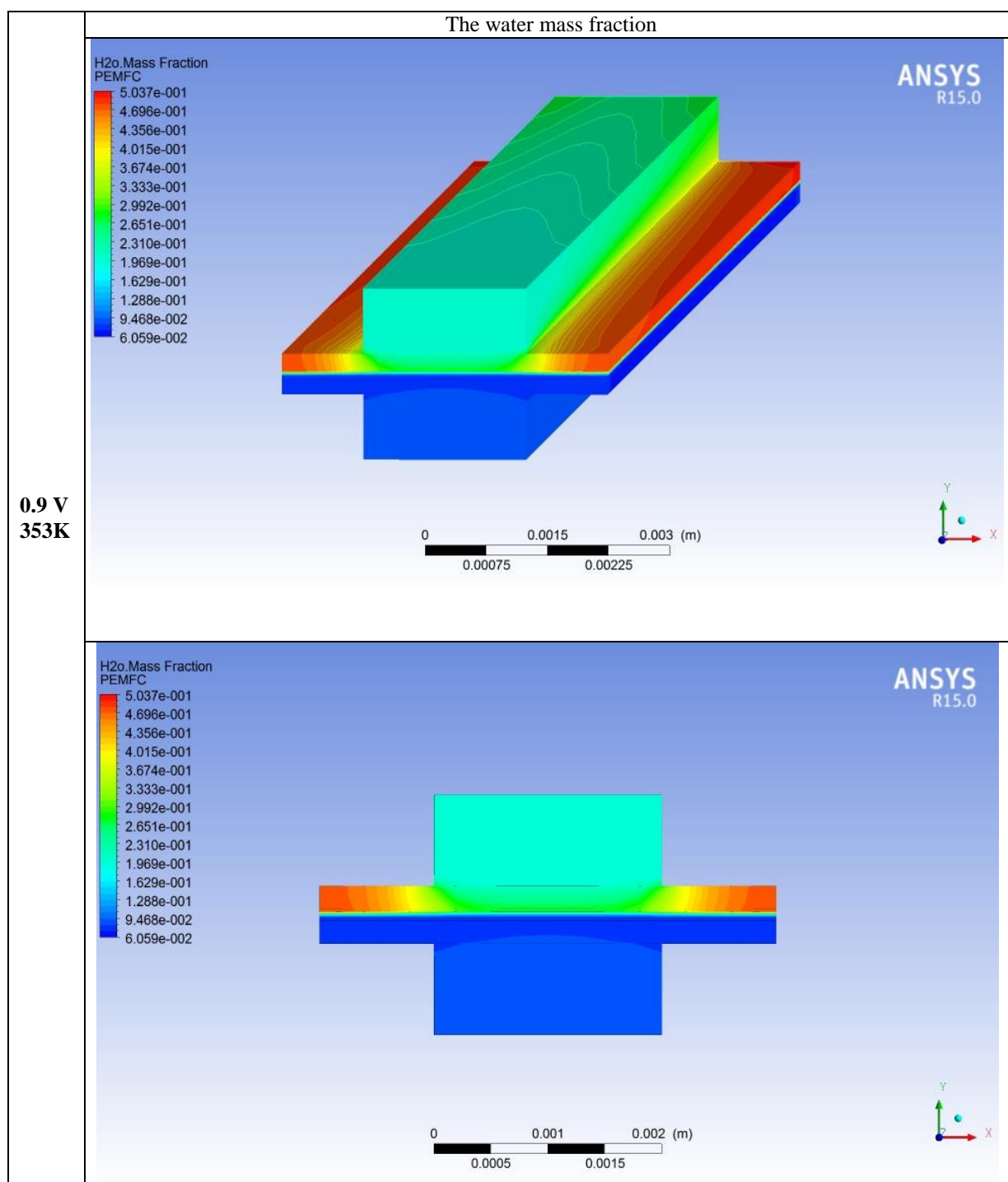


Figure 16. Water mass fraction distribution at 353 K, V= 0.9 V.

A comparison of the water mass fraction distribution and relative humidity at high voltage is presented in (Fig. 16) and (Fig. 17).

The water mass fraction generated is shown in (Fig. 16), at the cell inlet the water mass fraction is 0.22, and it increases to 0.28 at the outlet. As before, the majority of water generated in the cell is stagnating in the gas diffusion layer (GDL).

(Fig. 17) shows that the relative humidity is lower in the anode regions and membrane than in the

cathode regions. It can be seen that the relative humidity increases as the operation cell voltage decreases. The relative humidity is low at 0.9 V and high at 0.7 V. This behaviour is quite clear because at low cell voltages the chemical reaction rate becomes higher. Liquid water plays a key role in the hydrating membrane, but also it blocks the transport of oxygen to the cathode catalyst layer³¹. This factor has a negative effect on overall cell performance.

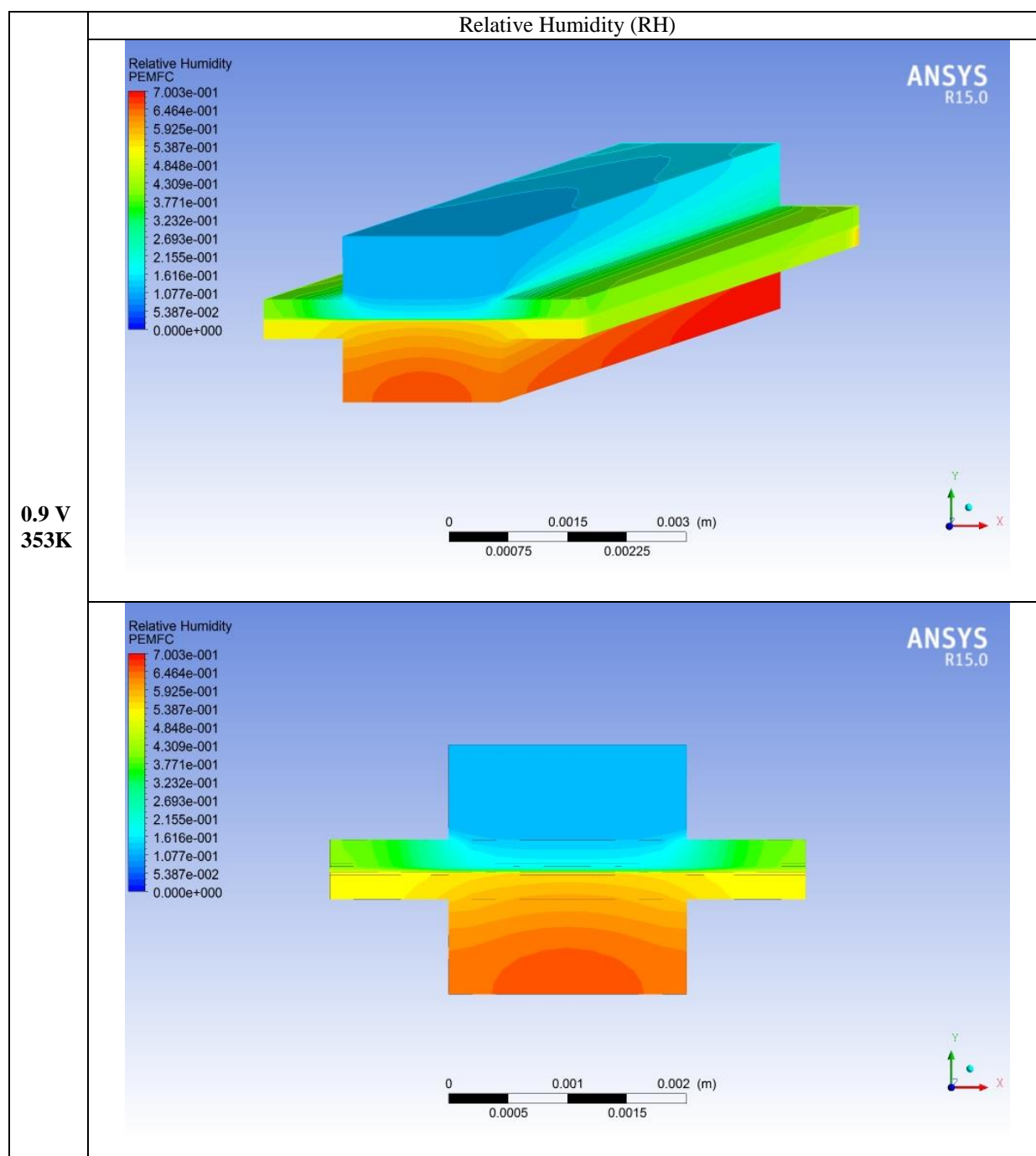


Figure 17. Relative humidity at 353 K, $V = 0.9$ V.

Conclusion

In this research paper, a thermo-fluid model is established to study the hydrogen and water dynamics in PEMFC. The simulation approach is validated by comparing our findings with the experimental results. The effects of temperature and cell voltage on the consumption of hydrogen are examined in this paper. The hydrogen mass fraction and water mass fraction are analyzed.

The results showed that:

- The amount of hydrogen decreases along the z-axis from plane 1 ($z=0$ mm) to plane 6 ($z=50$ mm).
- At 343 K, the mass fraction of hydrogen has significant decrease along the anode channel from the inlet to outlet by 19% at 0.7 V and 13% at 0.9 V.
- The hydrogen consumption was carried out by chemical reactions.
- There is high consumption of hydrogen at low cell voltages.
- The analysis of water production at the cathode side showed a high value of water content at low cell voltages.

Acknowledgements

We thank all the members of Research Team EMISys, Research Centre ENGINEERING 3S.

References

- 1- J. Brouwer, On the role of fuel cells and hydrogen in a more sustainable and renewable energy future, *Current Applied Physics*, **2010**, 10, 9-17.
- 2- J. Wang, H. Wang, Y. Fan, Techno-economic challenges of Fuel Cell Commercialization, *Engineering*, **2018**, 4, 352-360.
- 3- M. Reza Kazemi, I. Heydari, Z. Zhang, Hybrid systems: combining membrane and absorption technologies leads to more efficient acid gases (CO₂ and H₂S) removal from natural gas, *Journal of CO₂ utilization*, **2017**, 18, 362-369.
- 4- D.O. Akinyele, R.K. Rayudu, Review of energy storage technologies to sustain power networks, *Sustainable Energy Assess*, **2014**, 8, 74-91.
- 5- J.Y. Wang, Barriers of scaling-up fuel cells: cost, durability and reliability, *Energy*, **2015**, 80, 509-521.
- 6- M. Al-Baghdadi, H. Al-Janabi, Modeling optimizes PEM fuel cell performance using three-dimensional multi-phase computational fluid dynamics model, *Energy Convers. Manage*, **2007**, 48, 3102-3119.
- 7- J.H. Lin, W.H. Chen, Y.J. Su, T.H. Ko, Effect of gas diffusion layer compression on the performance in a proton exchange membrane fuel cell, *Fuel*, **2008**, 87, 2420-2424.
- 8- I. Tolj, M. Lototskyy, M. Davids, S. Pasupathi, G. Swart, B. Pollet, Fuel cell-battery hybrid powered light electric vehicle (golf cart): Influence of fuel cell on the driving performance, *International Journal of Hydrogen Energy*, **2013**, 38, 10630-10639.
- 9- J. T. Hinatsu, M. Faulkner, H. Takenaka, water uptake of perfluoro sulfonic acid membranes from liquid water and water vapour, *Journal of the electrochemical society*, **1994**, 141, 1493-1498.
- 10- E. Ozden, I. Tari, Proton exchange membrane fuel cell degradation: A parametric analysis using Computational Fluid Dynamics, *J. Power Sources*, **2016**, 304, 64-73.
- 11- H. F. Hashemi, S. Rowshanzamir, M. Reza Kazemi, CFD simulation of PEM fuel cell performance: effect of straight and serpentine flow fields, *Math Comput Model*, **2012**, 55, 1540-1557.
- 12- H. Mahayri, H. Hassanzadeh, M.S Afrouzi, Three-dimensional transient multiphase flow simulation in a dead end anode polymer electrolyte fuel cell, *Journal of molecular liquids*, **2017**, 225, 391-405.
- 13- H. K. Esfeh, A. Azarafza, M. K. A. Hamid, On the computational fluid dynamics of PEM fuel cells (PEMFCs): an investigation on mesh independence analysis, *RSC Adv.*, **2017**, 7, 32893-32902.
- 14- E. Hontañón, M.J. Escudero, C. Bautista, P.L. García-Ybarra, L. Daza, Optimisation of flow-field in polymer electrolyte membrane fuel cells using computational fluid dynamics techniques, *Journal of Power Sources*, **2000**, 86, 363-368.
- 15- W. Ying, M. Ouyang, Three-dimensional Heat and Mass transfer analysis in an air-breathing proton exchange membrane fuel cell, *Journal of Power Source*, **2007**, 164, 721-729.
- 16- H. Zhang, P. Pei, X. Yuan, The conception of the in-plate adverse-flow field for a proton exchange membrane fuel cell, *Int. J. Hydrog. Energy*, **2010**, 35, 9124-9133
- 17- Inc. ANSYS FLUENT 12.0 fuel cells module manual, April **2009**.
- 18- T.E. Springer, T.A. Zawodzinski, S. Gottesfeld, Polymer electrolyte fuel cell model, *Journal of the Electrochemical Society*, **1991**, 138, 2334-2342.
- 19- L. Wang, A. Husar, T. Zhou, H. Liu, A parametric study of PEM fuel cell performances, *Int. J. Hydrog. Energy*, **2003**, 28, 1263-1272.
- 20- A. Arvay, A. Ahmed, X.H. Peng, A.M. Kannan, Convergence criteria establishment for 3D simulation of proton exchange membrane fuel cell, *Int. J. Hydrog. Energy*, **2012**, 37, 2482-2489.
- 21- C.M. Baca, R. Travis, M. Bang, Three-dimensional, single-phase, non-isothermal CFD model of a PEM fuel cell, *J. Power Sources*, **2008**, 178, 269-281.
- 22- P. K. Takallo, E. S. Nia, M. Ghazi khan, Numerical and experimental investigation on effects of inlet humidity and fuel flow rate and oxidant on the performance on polymer fuel cell, *Energy Conversion and Management*, **2016**, 114, 290-302.
- 23- A. Awan, M. Saleem, A. Basit, Simulation of proton exchange membrane fuel cell by using ANSYS Fluent, *IOP Conf. Ser.: Mater. Sci. Eng*, 414, **2018**, 1-10.
- 24- A. Iranzo, M. Muñoz, J. Pino, F. Rosa, Update on a numerical model for the performance prediction of a PEM fuel cell, *Int. J. Hydrog. Energy*, **2011**, 36, 9123-9127.
- 25- T. Berning, N. Djilali, Three-dimensional computational analyses of transport phenomena in a PEM fuel cell, *Journal of Power source*, **2002**, 106, 284-294.
- 26- D.G. Sanchez, T. Ruiu, I. Biswas, K. A. Friedrich, J. S. Monreal, M. Vera, Effect of the inlet gas Humidification on PEMFC Behavior and Current Density Distribution, *ECS Trans.*, **2014**, 64, 603-617.
- 27- T. V. Nguyen, R. E. White, A water and thermal management model for proton exchange membrane fuel cells, *Journal of Electrochemical society*, **1993**, 140, 2178-2186.

- 28- J. Zhang, Y. Tang, C. Song, Z. Xia, H. Li, H. Wang, J. Zhang, PEM fuel cell relative humidity(RH) and its effect on performance at high temperatures, *Electrochimica Acta*, **2008**, 53, 5315-5321.
- 29- Y. Amadane, H. Mounir, A. El Marjani , Modeling the Temperature Effect on PEM fuel cell performance, *ICTEA* , Vol 2018 (2018), **2018**, 1-3.
- 30- E . Misran, N.S.M. Hassan, W.R.W. Daud, E.H. Majlan, M.I. Rosli, Water transport characteristics of a PEM fuel cell at various operating pressure and temperatures, *Int. J. Hydorg. Energy*, **2013**, 38, 9401-9408.
- 31- M. Ji, Z. Wei , A review of water management in Polymer Electrolyte Membrane Fuel Cells, *energies*, **2009**, 2, 1057-1106.